Inorg. Chem. **2005**, *44*, 1354–1361

A New Bimetallic Intercalated 3-D Assembly Magnet $[\{(323)Ni\}_3\{Fe^{III}(CN)_6\}_2]_n \cdot 12nH_2O$ (323 = *N,N′*-Bis(3-aminopropyl) Ethylenediamine): An Unprecedented Concomitant Presence of Meridional and Facial Arrangment of Ferricyanide Anion†

Manas K. Saha,‡ María C. Morón,§ Fernando Palacio,§ and Ivan Bernal*,‡

Department of Chemistry, University of Houston, Texas 77204, and Instituto de Ciencia de Materiales de Aragón, CSIC—Universidad de Zaragoza, 50009 Zaragoza, Spain

Received August 2, 2004

A novel molecular based magnet of three-dimensional (3-D) cyanide-bridged bimetallic assembly, $[\{(323)Ni\}_3\{Fe^{III}(CN)_6\}_2]_n \cdot 2nH_2O$ where 323 = *N,N′*-bis(3-aminopropyl) ethylenediamine, was synthesized and structurally characterized. The compound crystallizes in the orthorhombic space group *Pbca* with $a = 15.6560$ Å, $b = 15.2910$ Å, $c = 50.9120$ Å, and $Z = 8$. The assembly has two intercalated 3-D networks created by Fe^{III}–CN–Ni^{II}–NC–Fe^{III} linkages. The ferricyanide anion adopts both facial and meridional arrangements through the linkage. Interesting magnetic properties including 3-dimensional magnetic ordering were revealed. The assembly displays 3-dimensional magnetic ordering below 5.2 ± 0.1 K and field-induced magnetic behavior below 5.1 ± 0.1 K and above 1.15 ± 0.05 kOe.

Introduction

In recent years, considerable research has been done in the field of magnetic interactions between two paramagnetic metal ions through cyanide bridges.[1] This is especially true of the cyanide bridged 3-D bimetallic assemblies of Prussian blue type, derived from $[M(CN)_6]^{3-}$ (M = Cr, Fe) and simple transition metal ions $[M']^{n+}$, which are of potential interest because many of them exhibit a considerably high magnetic critical temperature.[2] However, magneto-structural correlation of these high T_C or T_N compounds remains unclear because of the difficulty of obtaining single crystals suitable for X-ray diffraction analysis. To overcome the problem, cyanide bridged extended bimetallic assemblies were obtained by the reaction of coordinately unsaturated transition metal complexes containing polydentate ligands $[M'L]^{m+}$ with hexacyanometalate building blocks $[M(CN)_6]^{3-}$ (M = Cr, Fe, or Mn). This hybrid approach favors suitable crystallization and therefore magneto-structural studies. Concomitantly, the introduction of organic ligands could lower the symmetry of the lattice and afford various molecular structures, depending upon the difference in steric hindrance and coordination mode of the ligands L. Up to now, a series of 0-,[3] 1-,[4] 2-,[5] or 3-dimensional[6] structures derived from hexacyanometalate ions and transition metal complexes with vacant coordination sites have been reported. One-dimensional assemblies were generally constructed by using two

* To whom correspondence should be addressed. E-mail: ibernal@uh.edu.

† Dedicated to Philipp Gütlich on the occasion of his 70th birthday.

‡ University of Houston.

§ CSIC—Universidad de Zaragoza.

(1) Dunbar, K. R.; Heintz, R. A. *Prog. Inorg. Chem.* **1997**, *45*, 283. Verdaguer, M.; Bleuzen, A.; Marvaud, V.; Vaissermann, J.; Seuleiman, M.; Desplanches, C.; Scuiller, A.; Train, C.; Garde, R.; Gelly, G.; Lomenech, C.; Rosenman, I.; Veillet, P.; Cartier, C.; Villain, F. *Coord. Chem. Rev.* **1999**, *192*, 1023. Fehlhammer, W. P.; Fritz, M. *Chem. Rev.* **1993**, *93*, 1243. Cernak, J.; Orendac, M.; Potocnak, I.; Chomic, J.; Orendacova, A.; Skorsepa, J.; Feher, A. *Coord. Chem. Rev.* **2002**, *224*, 51 and references therein.

(2) Gadet, V.; Mallah, T.; Castro, I.; Verdaguer, M.; Veillet, P. *J. Am. Chem. Soc.* **1992**, *114*, 9213. Mallah, T.; Thiebaut, S.; Verdaguer, M.; Veillet, P. *Science* **1993**, *262*, 1554. Entley, W. R.; Girolami, G. S. *Science* **1995**, *268*, 397. Entley, W. R.; Girolami, G. S. *Inorg. Chem.* **1994**, *33*, 5165. Ferlay, S.; Mallah, T.; Ouahes, R.; Veillet, P.; Verdaguer, M. *Nature* **1995**, *378*, 701. Kahn, O. *Nature* **1995**, *378*, 667. Sato, O.; Iyoda, T.; Fujishima, A.; Hashimoto, K. *Science* **1996**, *271*, 49. Verdaguer, M. *Science* **1996**, *272*, 698. Sato, O.; Iyoda, T.; Fujishima, A.; Hashimoto, K. *Science* **1996**, *272*, 704.

(3) Van Langenberg, K.; Batten, S. R.; Berry, K. J.; Hockless, D. C. R.; Moubaraki, B.; Murray, K. S. *Inorg. Chem.*, **1997**, *36*, 5006.

(4) (a) Ohba, M.; Maruone, N.; Okawa, H.; Enoki T.; Latour, J.-M. *J. Am. Chem. Soc.* **1994**, *116*, 11566. Ohba, M.; Fukita N.; Okawa, H. *J. Chem. Soc., Dalton Trans.* **1997**, 1733. (b) Ohba, M.; Usuki, N.; Fukita N.; Okawa, H. *Inorg. Chem.* **1998**, *37*, 3349. Fu, D. G.; Chen, J.; Tan, X. S.; Jiang, L. J.; Zhang, S. W.; Zheng, P. J.; Tang, W. X. *Inorg. Chem.* **1997**, *36*, 220. (c) Kou, H.-Z.; Liao, D.-Z.; Cheng, P.; Jiang, Z.-H.; Yan, S.-P.; Wang, G.-L.; Yao, X.-K.; Wang, H.-G. *J. Chem. Soc., Dalton Trans.* **1997**, 1503.

10.1021/ic048947f CCC: $30.25
Published on Web 01/22/2005

of the six cyanide groups of the hexacyanometalate, as bridging agents, and possess different types of structural motifs: rope-ladder-like chain,[4a] zigzag chain,[4b] etc. Some one-dimensional chains were observed that contain molecular squares,[4c] where more than two cyano groups are involved in bridging. An appreciable number of hexacyanometalate bimetallic assemblies possess a two-dimensional structure.[5] For $[M'L]_3[M(CN)_6]_2$ systems, containing *trans* metal macrocyclic complexes, two types of arrangements, facial and meridional, were observed for three bridging cyanide groups. The facial arrangement leads to a stair-shaped 2-D honeycomb network[5a] whereas the meridional arrangements lead to either a 2-D flat brick wall-like layer[5b] or a double chain stair-like[5c] structure. Well-characterized 3-D networks involving a hybrid approach of organic ligand metal complex and hexacyanometalate are limited. Probably the first 3-D bimetallic assemblies with a cubane network were reported by Fukita et al.,[7] but they showed no relevant magnetic properties due to the diamagnetic nature of Fe^{II}. Very recently, a new bimetallic assembly Ni_3Fe_2 was reported by Zhang et al.,[6b] possessing a 3D tunnel structure using ferricyanide anion as a building block. Since in systems with low magnetic anisotropy ferromagnetism is a three-dimensional property,[8] it would be logical to further explore the possibility of 3-D coupling in such systems.

Here we report on the crystal and magnetic properties of a new bimetallic three-dimensional assembly $[\{(323)Ni\}_3\{Fe^{III}(CN)_6\}_2]_n\cdot 12nH_2O$, **1**, where ferromagnetism does not arise spontaneously but is induced at rather small magnetic fields. The crystal structure determined by X-ray crystallography indicates a three-dimensional topology due to the unique presence of both facial and meridional stereoarrangements of the ferricyanide anion, as it provides cyano-bridges to the Ni-centers. Magnetic properties revealed that 3-dimensional ordering takes place with interesting metamagnetic properties.

Table 1. Crystallographic Data for $[\{(323)Ni\}_3\{Fe^{III}(CN)_6\}_2]_n\cdot 12nH_2O$

empirical formula	$C_{36}H_{90}Fe_2N_{24}Ni_3O_{12}$	cryst syst	orthorhombic
fw	1339.15	λ	0.71073 Å
space group	*Pbca*	ρ_{calc}	1.46 g cm^{-3}
a	15.656(2) Å	μ(Mo Kα)	1.445 cm^{-1}
b	15.291(2) Å	GOF	1.024
c	50.912(7) Å	R_{obs}	0.0651
V	12188(3) Å^3	R_{all}	0.1422
Z	8	$wR2_{obs}$	0.1153
T	100(2) K	$wR2_{all}$	0.1385

Experimental Section

The component complex $[(323)Ni(H_2O)_2]Cl_2\cdot 3H_2O$ was prepared by the literature method.[9] The salt $K_3[Fe(CN)_6]$ was purchased from Aldrich Chemical Co. was of reagent grade, and used as such.

$[\{(323)Ni\}_3\{Fe^{III}(CN)_6\}_2]_n\cdot 12nH_2O$, 1. An immediate precipitate of $[\{(323)Ni\}_3\{Fe^{III}(CN)_6\}_2]_n\cdot 12nH_2O$ is formed on mixing aqueous solutions of $K_3[Fe(CN)_6]$ (0.33 g, 1.0 mmol) in 20 mL of water and $[(323)Ni(H_2O)_2]Cl_2\cdot 3H_2O$ (0.30 g, 1.5 mmol) in 20 mL of water at room temperature. Subsequent slow interdiffusion of the two solutions in a U-tube gave prism-shaped orange crystals of $[\{(323)Ni\}_3\{Fe^{III}(CN)_6\}_2]_n\cdot 12nH_2O$ suitable for single-crystal X-ray diffraction. The compound is stable in air, and its composition by elemental analysis and infrared spectrum follow. Anal. Calcd for $C_{36}H_{90}Fe_2N_{24}Ni_3O_{12}$: C = 32.29, H = 6.77, N = 25.10. Found: C = 31.98, H = 6.46, N = 25.28. IR (cm^{-1} KBr disk) ν(CN) 2152, 2125, 2105. Yield, 0.60 g, ~90%.

X-ray Data Collection and Structure Refinement. Suitable crystals of **1** (prism, orange, dimensions 0.05 × 0.1 × 0.17 mm^3) were used for the structure determination. Data collection at 100 K was carried out with a Nonius CCD instrument using Mo Kα radiation. Data were corrected for absorption using SADABS.[10] The data were processed using the WinGx[11] package of programs. The structures were solved by direct methods in SIR-92[12] and SHELXS-86[13] and refined by full-matrix least-squares, based on F^2, using SHELXL-97.[14] All non-H atoms refined anisotropically by unit-weighted full-matrix least-squares methods. Some of the hydrogen atoms were included at calculated positions and refined in the riding mode, and some were located on residual density maps. Their positions were then fixed and refined in a riding mode. For **1**, convergence was reached at a final R1 = 0.0652 [for $I > 2\sigma(I)$], wR2 = 0.1392 (for all data), and 957 parameters, with allowance for the thermal anisotropy for all non-hydrogen atoms. Details of data collection and processing are given in Table 1.

Magnetic Study. The magnetic experiments were carried out in a Quantum Design MPMS SQUID magnetometer. The ac susceptibility data as a function of the temperature, $\chi_{ac}(T)$, were collected between 1.8 and 40 K while the magnetization measurements, $M(T)$, were taken in the range 1.8−320 K at 100 Oe. The amplitude of the alternate magnetic field used in the ac experiments was of 1 Oe, at a frequency of 10 Hz. During the hysteresis cycles, performed at 1.8 and 3.0 K, the magnetic field was changed between ±15 kOe. The magnetization data as a function of field, $M(H)$, were collected up to 50 kOe at temperatures ranging from 1.8 to

(5) (a) Colacio, E.; D-Vera, J. M.; Ghazi, M.; Moreno, J. M.; Kivekas, R.; Lloret, F.; S-Evans, H. *Chem. Commun.* **1999**, 987. Kou, H.-Z.; Gao, S.; Bu, W.-M.; Liao, D.-Z.; Ma, B.-Q.; Jiang, Z.-H.; Yan, S.-P.; Fan Y.-G.; Wang, G.-L. *J. Chem. Soc., Dalton Trans.* **1999**, 2477. Kou, H.-Z.; Gao, S.; Ma, B.-Q.; Liao, D.-Z. *Chem. Commun.* **2000**, 713. (b) Kou, H.-Z.; Gao, S.; Ma, B.-Q.; Liao, D.-Z.; *Chem. Commun.* **2000**, 1309. Ferlay, S.; Mallah, T.; Vaissermann, J.; Bartolome, F.; Veillet, P.; Verdaguer, M. *Chem. Commun.* **1996**, 2481. (c) Ohba, M.; Okawa, H. *Coord. Chem. Rev.* **2000**, *198*, 313 and references therein.

(6) (a) El Fallah, M. S.; Rentschler, E.; Caneschi, A.; Sessoli, R.; Gatteschi, D. *Angew. Chem., Int. Ed. Engl.* **1996**, *35*, 1947. Ohba, M.; Usuki, N.; Fukita, N.; Okawa, H. *Angew. Chem., Int. Ed.* **1999**, *38*, 1795. (b) Zhang, S.-W.; Fu, D.-G.; Sun, W.-Y.; Hu, Z.; Yu, K.-B.; Tang, W.-X. *Inorg. Chem.* **2000**, *39*, 1142.

(7) Fukita, N.; Ohba, M.; Okawa, H.; Matsuda, K.; Iwamura, H. *Inorg. Chem.* **1998**, *37*, 842.

(8) (a) Klenze, R.; Kanellakopulos, B.; Trageser, G.; Eysel, H. H. *J. Chem. Phys.* **1980**, *72*, 5819. (b) Griebler, W. D.; Babel, D. *Z. Naturforsch.* **1982**, *37b*, 832. (c) Gadet, V.; Bujoli-Doeuff, M.; Force, L.; Verdaguer, M.; El Malkhi, K.; Deroy, A.; Besse, J. P.; Chappert, C.; Veillet, P.; Renard, J. P.; Beauvillain, P. In *Molecular Magnetic Materials*; Gatteschi, D., Kahn, O., Miller, J. S., Palacio, F., Eds.; NATO ASI Series 198; Kluwer: Dordrecht, The Netherlands, 1990; p 281. (d) Palacio, F. In *Localized and itinerant molecular magnetism. From molecular assemblies to the devices*; Coronado, E., Delhaes, P., Gatteschi, D., Miller, J. S., Eds.; NATO-ASI: Tenerife, 1995; Kluwer: 1996; Vol. 321, p 5. (e) Palacio, F. *Mol. Cryst. Liq. Cryst.* **1997** *305*, 385.

(9) Do, J.; Jacobson, A. J. *Inorg. Chem.* **2001**, *40*, 2468.

(10) Sheldrick, G. M. *SADABS*; University of Göttingen: Göttingen, Germany, 1996.

(11) Farrugia, L. J. *J. Appl. Crystallogr.* **1999**, *32*, 837.

(12) Altomare, A.; Cascarano, G.; Giacovazzo, C.; Gualardi, A. *J. Appl. Crystallogr.* **1993**, *26*, 343.

(13) Sheldrick G. M. *SHELXS-86: Program for the Solution of Crystals Structures*; University of Göttingen: Göttingen, Germany, 1986.

(14) Sheldrick G. M. *SHELXL-97, Program for the Refinement of Crystal Structures*; University of Göttingen: Göttingen, Germany, 1997.

Table 2. Selected Bond Distances (Å) and Angles (deg) of $[\{(323)Ni\}_3\{Fe^{III}(CN)_6\}_2]_n \cdot 12nH_2O$

Bond Distances (Å)

Fe1−C9	1.929(5)	Fe2−C27	1.949(6)	Ni2−N12	2.106(4)
Fe1−C10	1.936(5)	Fe2−C28	1.958(5)	Ni2−N13	2.117(4)
Fe1−C11	1.934(5)	Ni1−N1	2.097(5)	Ni2−N14	2.094(4)
Fe1−C12	1.954(5)	Ni1−N2	2.111(4)	Ni2−N15	2.159(4)
Fe1−C13	1.941(5)	Ni1−N3	2.139(5)	Ni3−N18	2.116(4)
Fe1−C14	1.953(5)	Ni1−N4	2.105(4)	Ni3−N20	2.119(4)
Fe2−C23	1.964(6)	Ni1−N5	2.085(4)	Ni3−N21	2.080(5)
Fe2−C24	1.937(6)	Ni1−N9	2.071(4)	Ni3−N22	2.117(5)
Fe2−C25	1.947(5)	Ni2−N7	2.080(4)	Ni3−N23	2.119(4)
Fe2−C26	1.944(5)	Ni2−N11	2.111(4)	Ni3−N24	2.104(5)

Bond Angles (deg)

C9−Fe1−C10	85.4(2)	C26−Fe2−C27	90.1(2)	N11−Ni2−N13	173.84(2)
C9−Fe1−C11	89.6(2)	C26−Fe2−C28	90.3(2)	N11−Ni2−N15	86.35(2)
C9−Fe1−C12	77.2(2)	C27−Fe2−C23	88.3(2)	N12−Ni2−N11	94.15(2)
C9−Fe1−C13	93.4(2)	C27−Fe2−C28	89.1(2)	N12−Ni2−N13	82.19(2)
C9−Fe1−C14	88.4(2)	C28−Fe2−C23	92.3(2)	N12−Ni2−N15	87.26(2)
C10−Fe1−C12	92.3(2)	N1−Ni1−N2	91.28(2)	N13−Ni2−N15	98.38(2)
C10−Fe1−C13	177.5(2)	N1−Ni1−N4	94.88(2)	N14−Ni2−N13	90.85(2)
C10−Fe1−C14	96.0(2)	N1−Ni1−N3	174.14(2)	N14−Ni2−N15	91.75(2)
C11−Fe1−C10	88.4(2)	N2−Ni1−N3	83.00(2)	N14−Ni2−N11	92.96(2)
C11−Fe1−C12	88.7(2)	N4−Ni1−N3	90.84(2)	N14−Ni2−N12	172.75(2)
C11−Fe1−C13	89.5(2)	N4−Ni1−N2	173.84(2)	N18−Ni3−N22	91.20(2)
C11−Fe1−C14	175.1(2)	N5−Ni1−N1	90.92(2)	N18−Ni3−N20	177.52(2)
C13−Fe1−C12	88.8(2)	N5−Ni1−N2	90.49(2)	N18−Ni3−N23	86.10(2)
C13−Fe1−C14	86.1(2)	N5−Ni1−N3	87.89(2)	N20−Ni3−N23	93.08(2)
C14−Fe1−C12	93.5(2)	N5−Ni1−N4	89.52(2)	N21−Ni3−N20	91.78(2)
C24−Fe2−C23	94.3(2)	N7−Ni2−N12	90.25(2)	N21−Ni3−N22	91.9(2)
C24−Fe2−C25	85.9(2)	N7−Ni2−N14	91.40(2)	N21−Ni3−N24	93.2(2)
C24−Fe2−C26	87.3(2)	N7−Ni2−N15	173.94(2)	N21−Ni3−N23	172.8(2)
C24−Fe2−C27	176.9(2)	N7−Ni2−N13	86.75(2)	N21−Ni3−N18	89.26(2)
C24−Fe2−C28	92.6(2)	N7−Ni2−N11	88.31(2)	N22−Ni3−N20	91.02(2)
C25−Fe2−C23	91.7(2)	N9−Ni1−N1	91.70(2)	N22−Ni3−N23	82.63(2)
C25−Fe2−C27	92.3(2)	N9−Ni1−N4	90.95(2)	N24−Ni3−N18	91.29(2)
C25−Fe2−C28	175.9(2)	N9−Ni1−N3	89.44(2)	N24−Ni3−N23	92.5(2)
C26−Fe2−C23	176.9(2)	N9−Ni1−N5	177.30(2)	N24−Ni3−N22	174.34(2)
C26−Fe2−C25	85.8(2)	N9−Ni1−N2	88.76(2)	N24−Ni3−N20	86.40(2)

5.5 K. Finally, field-dependent ac susceptibility experiments, χ_{ac}-(H), were performed up to fields of 10 kOe at temperatures in the range 1.8−5.4 K.

Elemental analyses of carbon, hydrogen, and nitrogen were obtained from Galbraith Analytical Laboratories, 2323 Sycamore Drive, Knoxville, TN 37921-1750. Infrared spectra were measured on a Perkin-Elmer 983 G spectrophotometer using KBr pellets.

Results and Discussion

Crystal Structure. Figure 1 shows a perspective view of the assembly with the atom-numbering scheme. The water molecules and the hydrogen atoms are omitted. Selected bond distances and angles with their estimated standard deviations are listed in Table 2. The asymmetric system consists of two $[Fe(CN)_6]^{3-}$ anions and three $[(323)Ni]^{2+}$ cations. All three nickel(II) centers assume a slightly distorted, octahedral, NiN_6 chromophore. The two axial positions are occupied by cyano group nitrogens with the range of distances from 2.071 to 2.159 Å. The equatorial positions are occupied by the N_4 set of donor atoms from the 323 ligand, with Ni−N distances in the range 2.094−2.139 Å. The *cis* N−Ni−N angles range from 83.0° to 94.15°, and the trans N−Ni−N angles range from 173.9° to 177.5°, deviating from the ideal values of 90° and 180°, respectively. The iron centers in the $[Fe(CN)_6]^{3-}$ unit adopt a minimally distorted octahedral environment, and the *trans* C−Fe−C angles range between 175.83° and 177.8°, whereas the *cis* C−Fe−C varies between 85.40° and 93.50°. The Fe−C and C≡N distances are in the ranges 1.930−1.964 and 1.135−1.165 Å. The Fe−C≡N bond angles range from 172° to 179.8°. The two torsional angles for Ni1−NC−Fe1 are −111932(4)° and 4.794(1)°, and for Ni3−NC−Fe2 they are 59.464(3)° and −4.528(1)°. The torsional angles for Ni2−NC−Fe1 and Ni2−NC−Fe2 are −16.347(4)° and

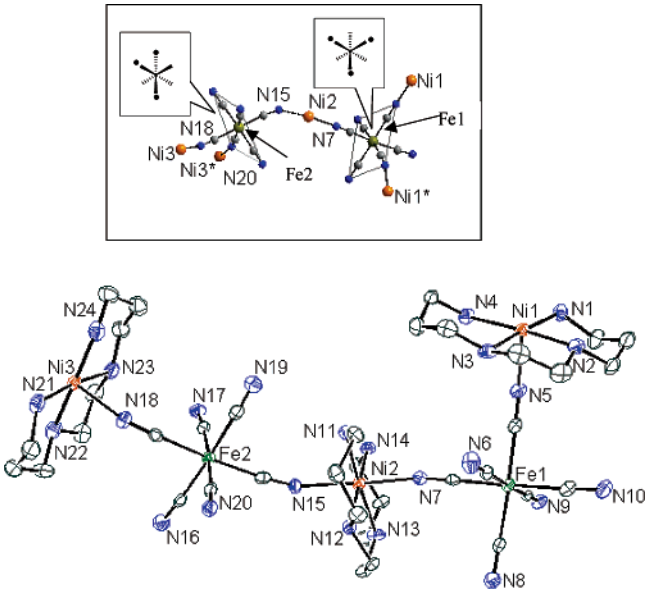

Figure 1. Crystallographic view of the asymmetric unit of **1**, H-atoms and water molecules are omitted for clarity. The inset shows the concomitant presence of merdional and facial arrangement of $[Fe(CN)_6]^{3-}$ unit.

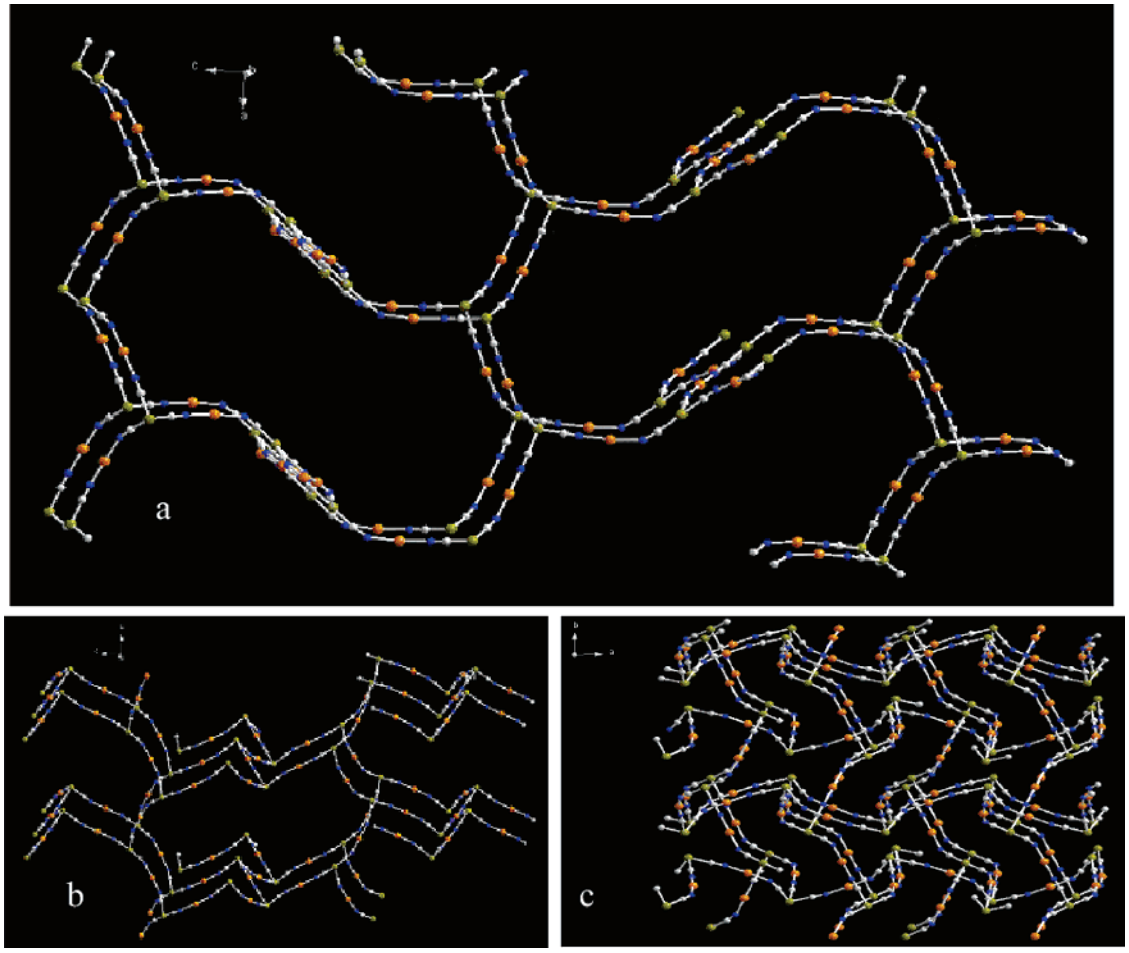

Figure 2. (a) The view of the 60 atom macrocyclic $[Fe1_6Fe2_4Ni1_4Ni2_4Ni3_2(CN)_{20}]$ unit, assembled in a 2-D network and propagating along the *b*-axis. (b) Propagation along the *a*-axis. (c) Propagation along the *b*-axis. (The 323 ligand, terminal cyanides, and water molecules are omitted for clarity.)

25.752(1)°, respectively. The two *trans* $CH_2-CH_2-CH_2-NH_2$ fragments of the 323 ligand possess a chair conformation.

Literature surveys show that, for cyanide bridged Ni_3M_2 systems, with three bridging and three nonbridging cyano groups, containing *trans* nickel macrocycle units, three different two-dimensional structures are possible depending on the arrangement of nickel macrocyclic units around the M ion. A facial arrangement leads to a corrugated 2-D honeycomb-like structure, whereas a meridional arrangement leads to either a 2-D flat brick wall-like layer or a double chain stair-like structure.[5] The simultaneous presence of both the facial and meridional arrangements has been demonstrated for the title complex, which is the first example of this type according to the best of our ability to scan the literature. In the inset of Figure 1, the arrangement of the bridging cyanides has been illustrated. Fe1 is in a facial arrangement, connected to apical sites of Ni1, Ni1*, and Ni2 through N5, N9, and N7 atoms, respectively, and Fe2 is in a meridional arrangement connected to apical sites of the Ni2, Ni3, and Ni3* though N15, N18, and N20, respectively. Three kinds of linkages, Fe1−CN−Ni2−NC−Fe2, Fe1−CN−Ni1−Fe1*, and Fe2−CN−Ni3−Fe2*, create the 60 atom macrocyclic $[Fe1_6Fe2_4Ni1_4Ni2_4Ni3_2(CN)_{20}]$ structure (depicted in Figure 2a), and the macro ring units are connected to each other through the facially linked $[Fe(CN)_6]^{3-}$. They are spread across the *ac* plane to construct a rare architecture of 2-D networks, as shown in Figure 2a. The 2-D architecture may be viewed as a 2-D assembly of the 1-dimensional rope-ladder chains.[4a] On the other hand, the meridionally arranged $[Fe(CN)_6]^{3-}$ links the macrocycle units in the direction parallel to the *b* axis and connects the 2-D sheets so as to form a 3-D structure, which may be visualized from Figure 2a. The three-dimensional propagation of the network along *a*, *b*, and *c* axes can well be illustrated by a joint examination of Figure 2a−c.

A closer observation into such an intricate network reveals that the ultimate, unique 3-D network is formed by the intercalation of two 3-D networks which are generated by the two sets of symmetry operations. They share the same topology but differ in the pattern of their proliferation, as they spread over the lattice. The intercalation of two networks is described by two different colors in Figure 3, where the red color signifies the network generated by the first set of symmetry operations and the olive color signifies the second set of symmetry operations. Note that the red and olive color 3-D networks are two crystallographically independent networks and, naturally, are not bonded to each other. However specifically colored macrocyclic units are connected among themselves, clarifying the intercalation of the two 3-D

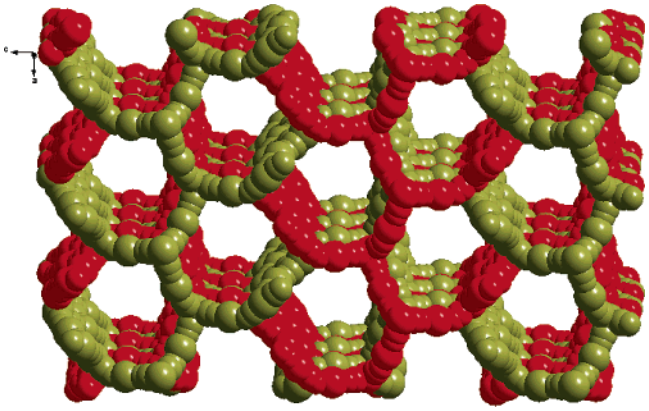

Figure 3. The two intercalated 3-dimensional networks (red and olive green), shown by a space-filling model. (The 323 ligand, terminal cyanides, and water molecules are omitted for clarity.)

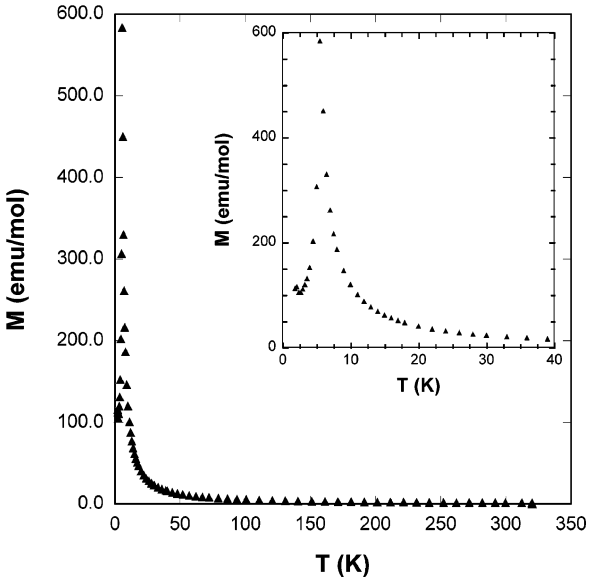

Figure 4. Temperature dependence of the magnetization of **1** at an external magnetic field of 100 Oe.

networks. The minimum distance between the strings of two intercalated network is 7.67 Å. For further understanding of the intercalation, please refer to the Supporting Information Figure 1 and Supporting Information Figure 2. This unique intercalation of two 3-D network arises by the fact that facial and meridional $[Fe(CN)_6]^{3-}$ anions link the nickel atom through cyano groups in different spatial arrangements. At this point, it should be mentioned that, for clarity, the projection of Figure 2 only illustrates one of the two networks that are intercalated. The water molecules are positioned in tunnels held by hydrogen bonding.

Magnetic Behavior: Paramagnetic Region. For **1**, the temperature dependence of the magnetization, $M(T)$, measured in an applied field of 100 Oe is shown in Figure 4. The data indicate that physical properties differ in two distinct temperature regions. Whereas at high temperature the behavior can be anticipated as paramagnetic, the rapid increase of the magnetization below about 30 K and the sharp peak at 5.4 ± 0.3 K suggest the presence of a phase transition to an ordered magnetic state. From these data, the dc magnetic susceptibility, χ, has been calculated as $\chi(T) = M(T)/H$. The

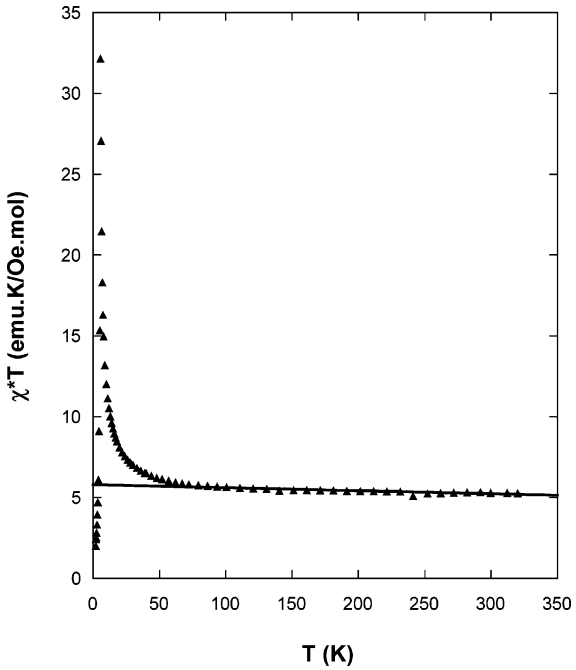

Figure 5. Evolution of χT with the temperature, where χ represents the dc magnetic susceptibility of **1**, collected at 100 Oe.

temperature dependence of χ^*T indicates a rapid increase of the experimental data at temperatures below 30 K (see Figure 5). An ideal paramagnetic compound is expected to follow the Curie law, $\chi = C/T$, and then the value of χ^*T should be temperature independent and equal to the Curie constant, C. If the temperature independent magnetic contributions, χ_{tim}'s, are not negligible, then $\chi^*T = C + \chi_{tim}{}^*T$, where χ_{tim} includes the diamagnetism of the compound, with diamagnetic contributions coming from the sample holder and the temperature independent paramagnetism arising from the paramagnetic ions. In the compound under study, above 100 K, the evolution of χ^*T versus T is linear with a negative slope that gives $\chi_{tim} = -0.0011$ emu/Oe mol. In the following analysis, the experimental data have been corrected from χ_{tim} contributions using such a calculated value.

The evolution of $1/\chi$ with temperature, shown in Figure 6, indicates that the compound behaves as a paramagnet at high temperature but deviates from the Curie law at lower value of T. The fit of the data to a Curie−Weiss law, $\chi(T) = C/(T - \theta)$, gives $C = 5.054$ emu·K/Oe·mol and $\theta = +5.13$ K for a fit performed between 30 and 320 K. In the paramagnetic region, the magnetism of this compound arises from the contribution of two iron and three nickel ions. The iron ions, $[Fe(CN)_6]^{3-}$, are in a low-spin state, $S_{Fe} = {}^1/_2$, while the Ni ions coordinate their four planar positions to the 3,2,3-tet ligand and the two axial ones coordinate to neighboring $[Fe(CN)_6]^{3-}$ counterions in a distorted octahedral symmetry. In this coordination, Ni^{2+} has $S_{Ni} = 1$ with typical values for the g-factor in the neighborhood of $g_{Ni} = 2.25$.[15] The Curie constant in such a system is formulated as

$$C = [N\mu_B{}^2/3k_B][2g_{Fe}{}^2S_{Fe}(S_{Fe} + 1) + 3g_{Ni}{}^2S_{Ni}(S_{Ni} + 1)] \quad (1)$$

Substitution of S_{Fe}, S_{Ni}, and g_{Ni} in eq 1 gives $g_{Fe} = 3.02$ in

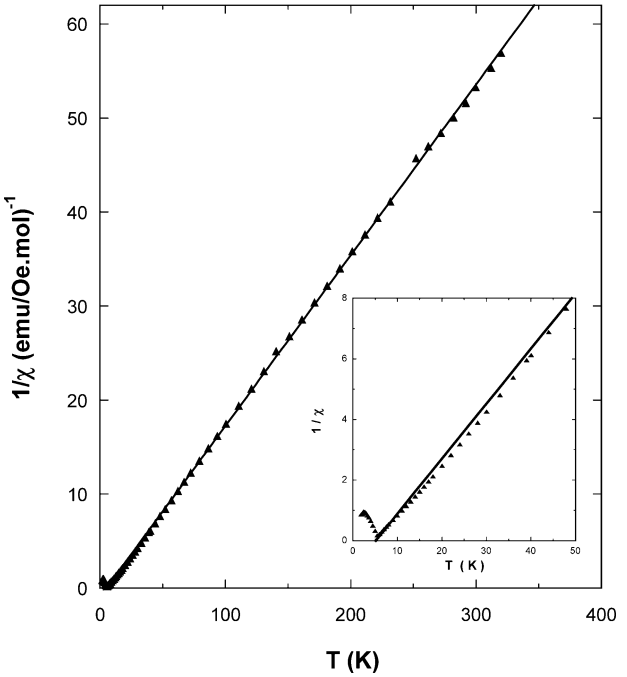

Figure 6. Temperature dependence of $1/\chi$, where χ stands for the dc magnetic susceptibility of **1**.

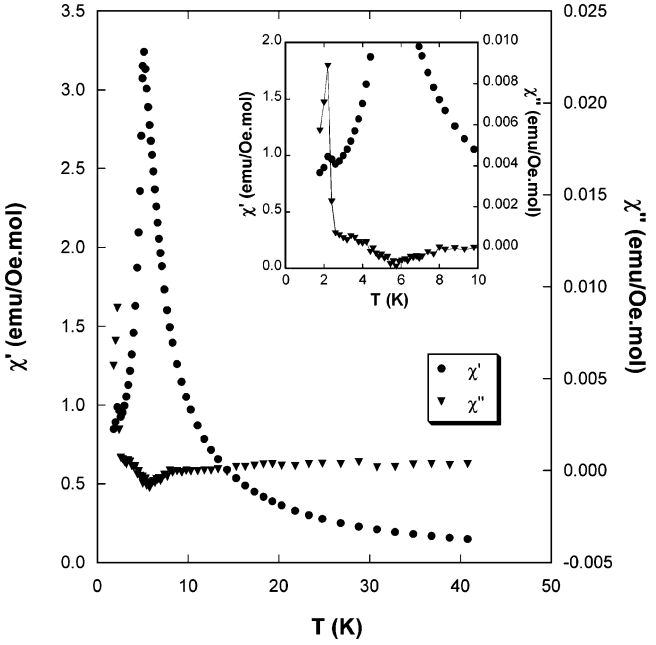

Figure 7. Temperature dependence of the ac magnetic susceptibility, χ_{ac}, of **1**.

good agreement with reported values for $[Fe(CN)_6]^{3-}$.[16] The positive value of the Curie−Weiss temperature indicates predominantly ferromagnetic interactions.

Magnetic Behavior: Ordered Magnetic Region. In order to investigate in detail the presence of magnetic ordering in **1**, ac susceptibility experiments as a function of temperature were carried out in zero applied magnetic field. The experimental data, depicted in Figure 7, show a peak at 5.2 ± 0.1 K in the in-phase component, χ', which is not followed by a peak in the out-of-phase component, χ'', of the susceptibility. This is of significant importance because the arising of net magnetization should be accompanied by the appearing of a signal in χ''.[8d,17] Therefore, it excludes the possibility of ferromagnetic ordering of **1**, showing that a positive value of θ indicates comparatively strong ferromagnetic interactions but does not necessarily imply that ferromagnetic ordering should arise. A sharp peak is observed in χ'' at about 2.2 K, accompanying a small feature in χ', see insert in Figure 7. It could be due to a small ferromagnetic impurity of unclear origin, whether extrinsic or due to the formation of minute amounts of a ferromagnetic chemical phase undetectable by the chemical analysis. Alternatively, it could also be due to the reorientation of the magnetic moments in the antiferromagnetic lattice although the low magnetic anisotropy of the ions rends this possibility very unlikely. Further experiments would be required to identify the origin of such an anomaly. In any case, since it has no influence either in the general magnetic behavior of the compound nor in the magnetization experiments discussed below we will not discuss it any further.

Under the influence of an external magnetic field and in the presence of competing interactions, systems that are antiferromagnetically ordered can exhibit a first-order transition to a phase characterized by the presence of a net magnetic moment. These materials are commonly referred as metamagnets.[8e,18] The compounds $FeCl_2$[19] and $[(CH_3)_3NH]CoCl_3 \cdot 2H_2O$[20] are two of the best-known examples of this type of behavior. In the absence of an applied magnetic field, the magnetic arrangement of the spins in these materials is characterized by a ferromagnetic coupling between the ions within a given crystallographic plane. These planes are weakly antiferromagnetically coupled. Then, the predominant magnetic interactions are ferromagnetic in character. However, these weak antiferromagnetic interactions are necessary to stabilize the antiferromagnetic ordering as the temperature is decreased. If an external magnetic field is applied in the antiferromagnetic state, the magnetic ordering is broken up at certain field values and the compound undergoes a first-order phase transition to a field-induced ferromagnetic state.

Magnetization versus applied magnetic field isotherms, collected for **1** between 1.8 and 5.5 K, indicate two different regimes as shown in Figure 8: at $T = 5.5$ and 5.0 K the magnetization isotherms show a monotonic increase that recalls a Brillouin-like function characteristic of the paramagnetic state. However, at 4.5 K and below, the magnetization isotherms are S-shaped curves compatible with a metamagnetic behavior are observed.[15] The difference can be clearly noted in Figure 9 where two isotherms are compared, each from a different temperature region. For all the temperatures considered, saturation of the magnetization

(15) Carlin, R. L. *Magnetochemistry*; Springer-Verlag: New York, 1986. Marvillers, A.; Parsons, S.; Riviere, E.; Audiere, J.-P.; Kurmoo, M.; Mallah, T. *Eur. J. Inorg. Chem.* **2001**, 1287.
(16) Figgis, B. N.; Lewis, J. *Prog. Inorg. Chem.* **1964**, *6*, 37.
(17) Palacio, F.; Lazaro, F. J.; van Duyneveldt, A. J. *Mol. Cryst. Liq. Cryst.* **1989**, *176*, 289.
(18) Stryjewski, E.; Giordano, N. *Adv. Phys.* **1977**, *26*, 487.
(19) De Jongh, L. J.; Miedema, A. R. *Adv. Phys.* **1974**, *23*, 1.
(20) Spence, R. D.; Botterman, A. C. *Phys. Rev. B* **1974**, *9*, 2993.

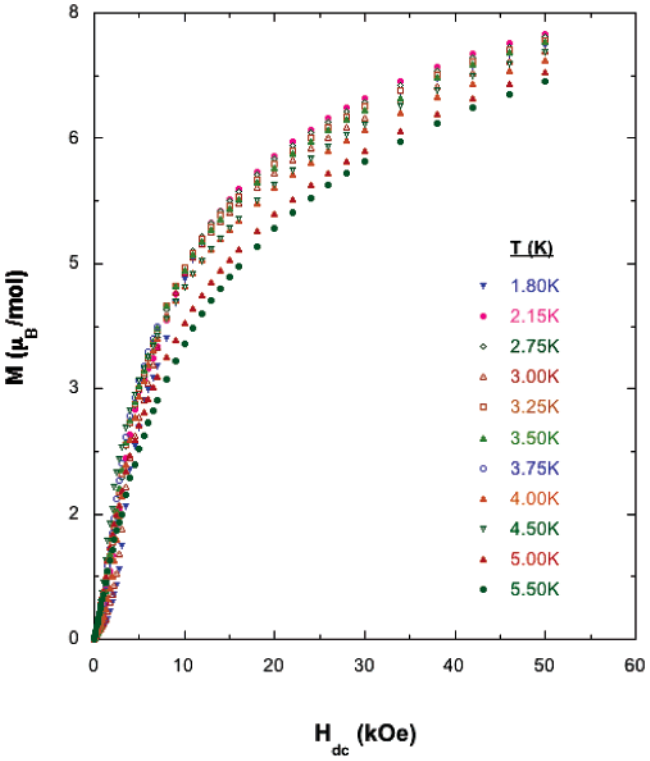

Figure 8. Magnetization isotherms of **1** above and below the magnetic ordering temperature.

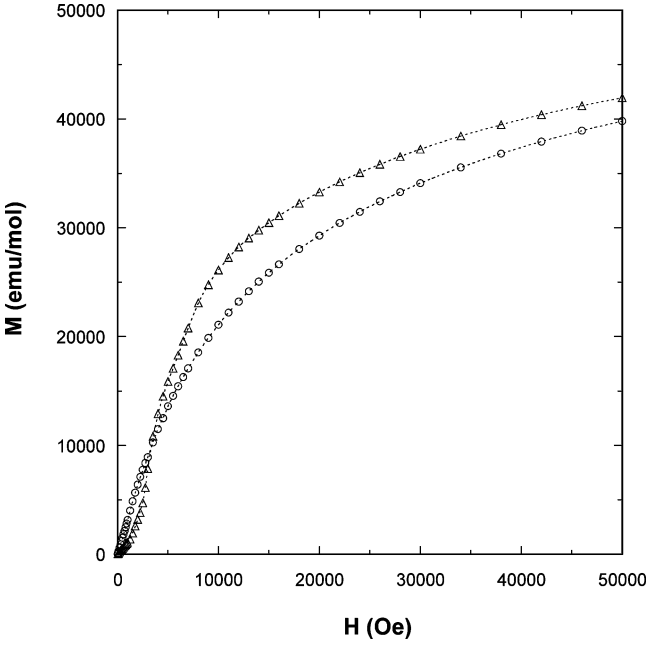

Figure 9. Magnetic field dependence of the magnetization of **1** at 3.0 K (△) and 5.5 K (○).

is not reached at the maximum experimental field applied, $H = 50$ kOe; instead, a maximum value of 7.7 μ_B/mol is measured at the lowest temperatures. Given that the total magnetization comes from the contribution of two Fe^{3+} ($S = {}^1/_2$, $g = 3.02$) and three Ni^{2+} ($S = 1$, $g = 2.25$) ions, a value of 9.77 μ_B/mol should be reached at saturation. Both the lack of saturation at 50 kOe and the maximum value of the measured magnetization at this magnetic field are in good agreement with previous observations in a related compound[5b,c]

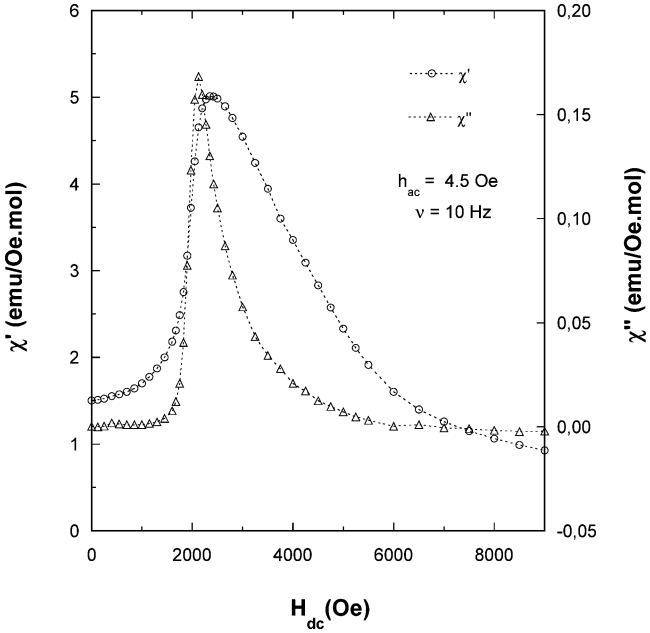

Figure 10. Magnetic field dependence of the ac magnetic susceptibility for **1** at 3.0 K.

and can be understood as due to the magnetic anisotropy of the compound, particularly of the low-spin iron ions. In particular, the magnetocrystalline anisotropy may force the respective orientations of the magnetic moments from ions belonging to different symmetry networks to move away from collinearity. Overcoming the effects of the magnetocrystalline anisotropy in order to *saturate* the magnetization in a completely parallel spin arrangement would require rather intense fields.

In order to investigate further the magnetic behavior of **1**, two different kinds of experiments have been performed. First, χ_{ac} data as a function of the applied magnetic field have been collected at temperatures between 1.8 and 5.4 K. A peak in both χ' and χ'' components can be observed for all the measured temperatures except at 5.4 K. A representative example is given in Figure 10 for the susceptibility isotherms at 3.0 K. They clearly indicate the presence of a field-induced transition to a magnetic state characterized by the presence of a net magnetic moment. That occurs for temperatures smaller than 5.1 ± 0.1 K. The critical magnetic field, estimated as the value corresponding to the maximum of χ', is $H_c = 2380 \pm 75$ Oe at 3.0 K. The temperature dependence of the critical magnetic fields, as determined from the $\chi_{ac}(H)$ isotherms, forms a boundary line of first-order phase transitions separating the antiferromagnetic phase from the field-induced ferromagnetic one. Such a line is shown in Figure 11. Moreover, the hysteresis cycle performed at 3.0 K (see Figure 12) also suggests the metamagnetic behavior of **1**. The lack of an abrupt increase of the magnetization at H_c, as it would correspond to the first-order phase transition from the antiferromagnetic state to the field-induced ferromagnetic state, is due to the fact that the experiments had to be made using powder samples.

The magnetic interaction propagates through pathways of the type −Fe−C−N−Ni−N−C−Fe−, with Fe−Ni distances

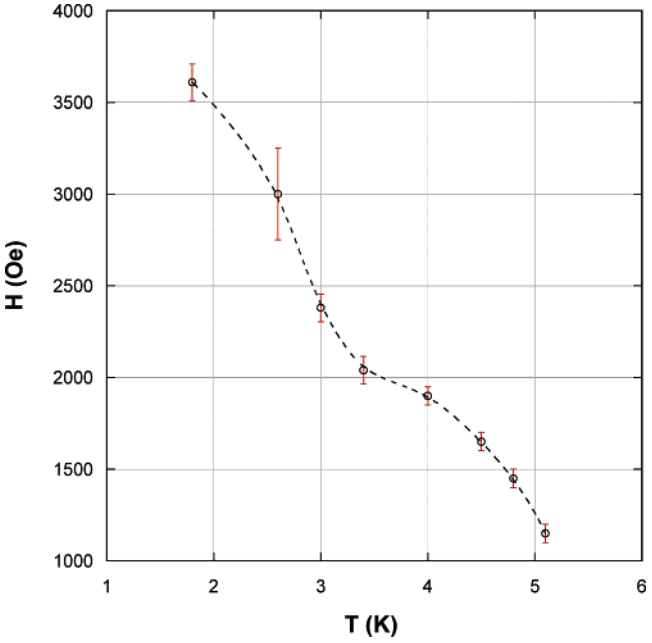

Figure 11. Temperature dependence of the applied magnetic field *H* required for inducing a net magnetic moment in Ni_3Fe_2.

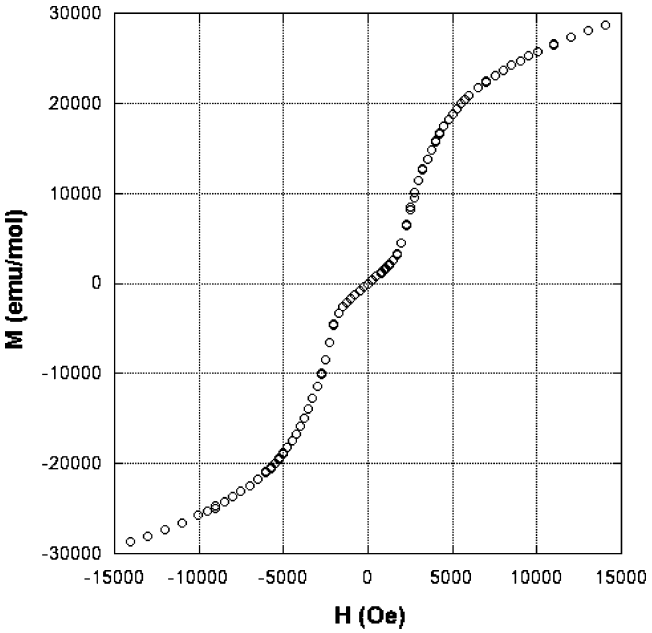

Figure 12. Magnetic hysteresis cycle for Ni_3Fe_2 at 3.0 K.

in the range 5.14−5.29 Å. Similar superexchange pathways can be observed in other 1-D and 2-D cyanide-bridged Ni_3Fe_2 assemblies.[5c] Magnetic interactions are always found to be ferromagnetic as corresponds to the strict orthogonality of t_{2g} (low spin Fe^{III}) and e_g (Ni^{II}) orbitals. When present, magnetic ordering is not always found to be ferromagnetic. An antiferromagnetic ground state that gives place to a ferromagnetic state through a metamagnetic phase transition at relatively low applied magnetic fields has been described for some 1-D and 2-D Ni_3Fe_2 compounds. The magnetic behavior of **1** shows that 3-D cyanide-bridged Ni_3Fe_2 assemblies can also lead to metamagnetism.

It is interesting to discuss the possible origin of metamagnetism in **1**. As explained above, the structure of **1** is formed by the intercalation of two symmetrically independent networks not bonded to each other. At Tc, each network becomes ferromagnetic although they orient antiferromagnetically with respect to each other. It would be difficult to suggest any particular origin for the antiferromagnetic internetwork interactions, whether through space exchange or dipolar, although it is anticipated that they will be rather weak. The application of a magnetic field will align both network magnetizations parallel, as soon as the magnetic energy overcomes the antiferromagnetic exchange interaction. For a magnetic field of 1.15 kOe at 5.1 K, a value of $J'/k = -0.012$ K can be estimated. Due to the intricate crystal structure of Ni_3Fe_2, neutron diffraction experiments can be helpful in providing a more detailed model for the particular arrangement of spins in this material. However, due to the tiny size of the crystals, we can go no further to that. However, the antiferromagnetic orientation of the two intercalated 3-D network with a minimum distances of 7.67 Å is supported by the conclusion drawn by Ohba et al.,[21] that for the 2-D network interchain spin coupling occurs when the interlayer separation is less than ∼10 Å.

Acknowledgment. We thank the Robert A. Welch Foundation for support of these studies (Grant 592 to I.B.), and for postdoctoral support to M.K.S., M.C.M., and F.P., we acknowledge the Comision Interministerial de Ciencia y Tecnologia (Grant MAT2001-3507-C02-02) for the support.

Supporting Information Available: Crystallographic data in CIF format and additional figures. This material is available free of charge via the Internet at http://pubs.acs.org.

IC048947F

(21) Ohba, M.; Okawa, H.; Ito, T.; Ohto, A. *J. Chem. Soc., Chem. Commun.* **1995**, 1545. Ohba, M.; Okawa, H.; Fukita, N.; Hashimoto, Y. *J. Am. Chem. Soc.* **1997**, *119*, 1011.